

Research Article

The Effect of Chirped Intense Femtosecond Laser Pulses on the Argon Cluster

H. Ghaforyan,¹ R. Sadighi-Bonabi,² and E. Irani²

¹Department of Physics, Payame Noor University, P.O. Box 19395-3697, Tehran, Iran

²Department of Physics, Sharif University of Technology, P.O. Box 11365-9567, Tehran, Iran

Correspondence should be addressed to R. Sadighi-Bonabi; sadighi@sharif.ir

Received 1 August 2016; Revised 2 October 2016; Accepted 12 October 2016

Academic Editor: Ming Liu

Copyright © 2016 H. Ghaforyan et al. This is an open access article distributed under the Creative Commons Attribution License, which permits unrestricted use, distribution, and reproduction in any medium, provided the original work is properly cited. The publication of this article was funded by SCOAP³.

The interaction of intense femtosecond laser pulses with atomic Argon clusters has been investigated by using nanoplasma model. Based on the dynamic simulations, ionization process, heating, and expansion of a cluster after irradiation by femtosecond laser pulses at intensities up to 2×10^{17} Wcm⁻² are studied. The analytical calculation provides ionization rate for different mechanisms and time evolution of the density of electrons for different pulse shapes. In this approach, the strong dependence of laser intensity, pulse duration, and laser shape on the electron energy, the electron density, and the cluster size is presented using the intense chirped laser pulses. Based on the presented theoretical modifications, the effect of chirped laser pulse on the complex dynamical process of the interaction is studied. It is found that the energy of electrons and the radius of cluster for the negatively chirped pulses are improved up to 20% in comparison to the unchirped and positively chirped pulses.

1. Introduction

Developments of ultrashort intense laser pulses through CPA and OPCPA techniques have attracted increasing attention in the main subject of laser-matter interaction [1]. These pulses are used for the generation of quasi monoenergetic electron beams up to megaelectron volts [2–6]. The ponderomotive force of laser accelerates plasma electrons to the relativistic energies over several MeV. In recent years, considerable progress has been made in increasing energy and quality of electron beams [7, 8].

High-energy electrons have various applications, including fast ignition of fusion reaction [9], production of intense radiation sources such as X-ray, dynamics of photochemistry, ionization and dissociation process, and biological and medical technology [10–14]. Optimization and control of this new source of energetic particles with different applications are a subject of current significance which can be modified by unique attractive techniques. One of the efficient attractive methods, interaction of intense laser pulses with large atomic clusters, has opened up several areas of laser plasma

science such as electron and ion accelerators [15–17], table-top neutron sources [18], plasma waveguides [19], and X-ray sources [20–22]. Simulation of this interaction not only is scientifically very interesting but also has a wide range of applications. One of the most important applications of laser-cluster interaction is particle acceleration. Low price and low space at the laser-plasma accelerators compared with other accelerators have led to more attention to this type of accelerator.

Although a target cluster which is made by high-pressure gas nozzle shows important properties such as solid-like electron density in some places, the average density of clusters is low. The transmission distance in the cluster is longer than that in the gas target. In addition, the absorbed laser energy in the cluster is larger than the solid and gas targets [23, 24]. Therefore, clusters have unique properties because they have the advantage of both the gas and solid phases. Another outstanding advantage of clusters in particle accelerations is their capability for controlling the dynamic of interaction of cluster by a laser pulse.

Simulation of laser interaction with large clusters possesses a great challenge. A fully ab initio treatment or molecular dynamics method is not feasible. A good approximation for clusters with an atomic number greater than 10000 atoms is one which considers the cluster as a nanoplasma medium. This model was developed in 1996 by Ditmire and his colleagues [25]. Nanoplasma model successfully justifies all phenomena in the interaction. Several improvements in the nanoplasma models have been made which are in good agreement with experimental results [26]. The pulse shaping techniques and application of chirped pulses have impressively improved controlled laser-plasma coupling [27]. Recently, chirping of short laser pulses has been recognized as a main parameter that can be used to control the dynamics of a system interacting by ultrafast laser pulses. However, there has been much less investigation on the chirp-dependent behavior of dynamics of molecular ionization. Levis and coworkers used optimized laser pulse with intensity of 10^{13} Wcm^{-2} to control the dissociation patterns in large molecules through various Stark-shifting electronically excited states into resonance condition [28]. Recently, Moll et al. reported the effect of excitation and deexcitation processes on the dynamic of laser-cluster interaction. They found that, with considering the excited states, the ionization dynamics is accelerated and the higher ionic charge states are reached at the end of the laser-cluster interaction. Moreover, the temperature of generated electron is reduced and the free electron density is increased due to the enhanced ionization dynamics [29]. Fukuda and coworkers demonstrated that energetic particle emissions from laser-cluster interactions are optimized by manipulating the sign of chirp [30]. Several theoretical models have been proposed to explain the mechanism of the production of highly energetic particles. However, due to the complex dynamical processes of the laser-cluster interaction, a comprehensive model has never been presented to explore the optimal conditions. To the best of our knowledge, there is no theoretical executive report on chirp-dependent behavior of complex dynamics of laser-cluster interaction using nanoplasma model. The main focus of this work is to investigate the effect of chirped intense femtosecond laser pulses on the dynamic of Argon cluster which is not tackled in the literature. In this work, a useful theoretical model is used which can properly elucidate the reported experimental results. In order to clarify the laser-cluster interaction, electron and ion density, electron energy, and radius of cluster are modified by manipulating the characters of laser fields, such as intensity, pulse duration, and chirp parameter via using nanoplasma model.

The aim is to improve the acceleration of particles by considering the modified negatively chirped pulse shapes. Indeed, the effect of chirped pulses creates some modifications on the current calculation models. The effect of chirped pulses in different intensities is also compared. Another feature of this work is to study the time evolution of the density of electrons and ions at different pulse shapes and the results are compared with near transform limited (unchirped) pulses. In addition, the effect of laser intensity, pulse duration, and the laser pulse shape has been investigated on the electron energy, charge state of ions, and cluster size. When we use

the negatively chirped laser pulse, it is found that the energy of electrons and radius of cluster are improved about 20% and 18% compared to the Gaussian pulse and positively chirped pulse, respectively. This is described in detail in the following.

This paper is organized as follows: in Section 2, the theory of laser-cluster interaction, the mechanisms of cluster ionization, cluster heating, and cluster expansion, and the ponderomotive force effect are described to provide the effective parameters at laser-cluster interaction; in Section 3, the simulation results are explained in detail; and the paper is concluded in Section 4.

2. Theory of Laser-Cluster Interaction

Various models are used to describe the interaction of lasers with atomic clusters. These models include the coulomb explosion model [31], the ionization ignition model [32], the inner shell excitation [33], and nanoplasma model [25–33]. The most successful method for studying the dynamical evolution of large clusters under strong fields is the nanoplasma model.

In this model, cluster atoms are ionized by the incident laser pulse (inner ionization) and form a nanoplasma sphere. Quasi-free electrons participate in an oscillation that is created by the laser field and interact with other particles. Electron-impact ionization of the cluster produces additional free electrons and vacancies in inner shell which are the origin of the X-ray radiation. Fraction of the electrons finds enough energy to escape from the cluster (external ionization) and leaves behind a net positive charge. The cluster, then, expands in response to coulomb explosion and hydrodynamic forces. The enhancement of the laser intensity makes ponderomotive force as an important component of the interaction dynamics. However, there are three main processes (ionization, heating, and expansion) in the nanoplasma model that is discussed in detail.

2.1. Cluster Ionization Mechanism. When the rising edge of the laser pulse reaches the cluster, ionization of the cluster begins and a small number of quasi-free electrons are generated. This is called the tunnel ionization and the rate of tunnel ionization is described in this model by ADK formula that is given by [34]:

$$W_{\text{ADK}} = \omega_a \frac{(2l+1)(l+|m|)!}{2^{|m|}|m|!(l-|m|)!} \left(\frac{2e}{n^*}\right)^{n^*} \frac{1}{2\pi n^*} \cdot I_p \left(\frac{2E}{\pi(2I_p)^{3/2}}\right)^{1/2} \left(\frac{2(2I_p)^{3/2}}{E}\right)^{2n^*-|m|-1} \cdot \exp\left[-\frac{2(2I_p)^{3/2}}{3E}\right], \quad (1)$$

where the constant e is Euler's number, $n^* = Z[2I_p]^{-1/2}$ is the effective principal quantum number, ω_a is the atomic frequency ($\omega_a = 4.13 \times 10^{16} \text{ s}^{-1}$), I_p is the ionization potential of charge state, and E is the field of laser in atomic units.

The second ionization mechanism in the cluster occurs in inelastic collisions between electrons and ions. A few electrons produced by optical ionization collide with atoms inside the cluster and create another ionization that is called collisional ionization. The production of higher charge states is dominated by collisional ionization as a result of the high density in the cluster. Rate of collisional ionization in nanoplasma model is calculated by the Lotz equation [35]:

$$W_{\text{col}} = n_e \frac{a_i q_i}{I_p (kT_e)^{1/2}} \int_{I_p/kT}^{\infty} \frac{e^{-x}}{x} dx. \quad (2)$$

Here, n_e is the electron density, I_p is the ionization potential in eV, q_i is the number of electrons in the outer shell of the ion, and a_i is an empirical constant equal to $4.5 \times 10^{-14} \text{ eV}^2 \text{ cm}^{-3}$.

In addition to the thermal energy, the electrons in the cluster have a velocity associated with their oscillations in the laser field. Oscillation of the electrons by the laser field leads to another ionization which is given as follows [36]:

$$W_{\text{las}} \approx n_e \frac{a_i q_i}{2\pi I_p m_e^{1/2} U_p^{1/2}} \left\{ \left[3 + \frac{I_p}{U_p} + \frac{3}{32} \left(\frac{I_p}{U_p} \right)^2 \right] \cdot \ln \left[\frac{1 + \sqrt{1 - I_p/2U_p}}{1 - \sqrt{1 - I_p/2U_p}} \right] - \left(\frac{7}{2} + \frac{3I_p}{8U_p} \right) \cdot \sqrt{1 - I_p/2U_p} \right\}. \quad (3)$$

Hence, the ionization rate of the laser-cluster interaction is equal to

$$W = W_{\text{ADK}} + W_{\text{col}} + W_{\text{las}}. \quad (4)$$

It becomes clear from the results of this research and previous studies that dominant ionization in laser-cluster interaction is collisional ionization. At the same time, three-body recombination occurs and reduces the number of electrons and increases the temperature of the system. The rate of three-body recombination, α_3 , is [37]

$$\alpha_3 = \frac{4\pi\sqrt{2\pi}}{9} \frac{e^{10} Z^3}{m_e^{1/2} (kT_e)^{9/2}} \ln \sqrt{1 + Z^2}. \quad (5)$$

Here, Z is charge state of cluster.

2.2. Cluster Heating Mechanism. In the hydrodynamic model, the laser deposits energy into the cluster through inverse bremsstrahlung. The plasma is treated as a dielectric medium, and the Drude model gives its dielectric constant as follows:

$$\varepsilon = 1 - \frac{\omega_p^2}{\omega(\omega + iv)}. \quad (6)$$

The applied electric field is assumed to be uniform all over the plasma (the cluster radius is on the order of 15 nm, and the wavelength of light is 825 nm), and the electric field inside the cluster is given by [38]

$$E = \frac{3}{|\varepsilon + 2|} E_{\text{ext}}, \quad (7)$$

where E_{ext} is laser field outside the cluster. The rate of energy deposition by an applied electric field into a dielectric is given by

$$\frac{\partial U}{\partial t} = \frac{1}{4\pi} \vec{E} \cdot \frac{\partial \vec{D}}{\partial t}. \quad (8)$$

By placing electric field inside the cluster, we get

$$\begin{aligned} \frac{\partial U}{\partial t} &= \frac{9\omega}{4\pi} \frac{\text{Im}[E]}{|\varepsilon + 2|^2} |E_{\text{ext}}|^2 \\ &= 7312.5\omega \text{Im}[E] |E|^2 \text{ eV} / (\text{nm}^3 \text{ fs}), \end{aligned} \quad (9)$$

where E is field inside the cluster in atomic unit. The inverse bremsstrahlung (IBS) absorption (or collisional) rate for a clustered plasma is given by

$$Q = \frac{\omega_p^2 \text{Re } \nu(\omega)}{[\omega - \omega_p^2/3\omega - \text{Im } \nu(\omega)]^2 + [\text{Re } \nu(\omega)]^2} \frac{|E_0|^2}{8\pi}. \quad (10)$$

Here, $|E_0|^2$ is proportional to the intensity of the laser and $\nu(\omega)$ is the collision frequency.

The electron temperature equation inside the cluster is [39]

$$\frac{\partial T_e}{\partial t} = \frac{2}{3} \frac{Q}{n_e} - \frac{T_e}{n_e} \frac{dn_e}{dt} + \frac{2}{3} \cdot \sum_{Z=0}^{\infty} \varepsilon_i(Z) [\alpha_3(Z+1) n_e n_i(Z+1) - S(Z) n_i(Z)]. \quad (11)$$

Here, n_e is the electron density and S is the collisional ionization rate coefficient, which are effective parameters in electron temperature. After the initial ionization, the electron density in the cluster plasma is much larger than the critical density for 825 nm laser wavelength. However, as the cluster expands, the density falls and the real part of the dielectric constant, which initially has a large negative value, approaches -2 .

2.3. Cluster Expansion Mechanism. Cluster expansion is the result of the coulomb pressure and hydrodynamic pressure in the nanoplasma model. Coulomb pressure is the result of the repulsive ions that occur in clusters and can be found by the following equation [40]:

$$P_{\text{coul}} = \frac{Q^2 e^2}{8\pi r^4}. \quad (12)$$

Here, r is the radius of the cluster. The hydrodynamic pressure created as a result of the expansion of the hot electrons is given by

$$P_e = n_e kT_e. \quad (13)$$

Here, n_e is the electron density, T_e is the electron temperature, and k is the Boltzmann constant.

2.4. Ponderomotive Force. Due to the effect of the chirped pulses, some modifications are made on the current calculation models. When a beam of high-power laser radiation is used to heat the plasma, radiation pressure becomes significant. Electrons in plasma are accelerated to relativistic energies with ponderomotive force of laser light. In hydrodynamic model, plasma dynamics are driven predominantly by the hydrodynamic pressure and the ponderomotive pressure. The enhancement of the laser intensity at the critical density surface makes ponderomotive forces an important component of the plasma dynamics. The equation of motion of electrons in the presence of an EM wave is described by

$$\vec{F}_L = m \frac{d\vec{v}}{dt} = -e \left(\vec{E}(\vec{r}, t) + \frac{1}{c} \vec{U} \times \vec{B}(\vec{r}, t) \right), \quad (14)$$

where $\vec{E}(\vec{r}, t)$, \vec{U} , and $\vec{B}(\vec{r}, t)$ are the electric field, electron velocity, and magnetic field, respectively. The electric field is given by

$$\vec{E}(\vec{r}, t) = \vec{E}_s(\vec{r}) f(t) \cos \omega_0 t. \quad (15)$$

Here, $f(t)$ and ω_0 denote the temporal profile and the carrier frequency, respectively. A Gaussian envelope of $f(t)$ is given by

$$f(t) = \exp \left[-\frac{2 \ln 2 t^2}{\tau^2} \right], \quad (16)$$

where τ is FWHM time duration. Linearly chirped laser field can be defined as follows:

$$E(t) = E_0 \exp \left\{ -\left(1 + ib\right) \left(\frac{t \sqrt{2 \ln 2}}{\tau_L} \right)^2 \right\}, \quad (17)$$

where b and τ_L are the chirp parameter and pulse duration. $b > 0$ means a positive chirp and $b < 0$ means a negative chirp. Laser intensity of the chirped laser pulse is expressed as follows:

$$I(t) = I_0 \exp \left\{ \left[-\frac{t^2}{2\tau^2} \right] \left[1 + \frac{bt}{(t^2 + \tau^2)^{1/2}} \right]^{-1} \right\}, \quad (18)$$

where I_0 denotes the peak laser intensity of the near transform limited pulse. By using a second-order approximation and expansion of E around r_0 , the force exerted on an electron can be obtained as follows:

$$\vec{F}_{NL} = -\frac{\omega_p^2}{8\pi\omega_0^2} \vec{\nabla} \langle \vec{E}^2 \rangle. \quad (19)$$

Although this force essentially enters the electrons, in the end, it is transmitted to the ions too. When electrons are classified by \vec{F}_{NL} , a field separator (\vec{E}_{es}) is produced. Therefore, the total force exerted on the electrons would be as follows:

$$\vec{F}_e = -e\vec{E}_{es} + \vec{F}_{NL}. \quad (20)$$

Indeed, the ponderomotive force is very important for accelerating the electrons.

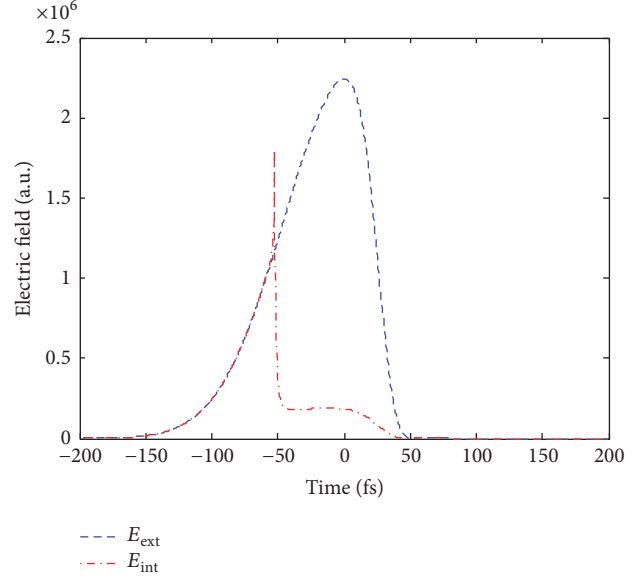


FIGURE 1: The electric field inside the cluster and external negatively chirped laser pulse field with 40 fs duration pulse, $6 \times 10^{14} \text{ Wcm}^{-2}$ laser intensity, and 825 nm wavelength.

3. Simulation Results

Calculations are carried out for Argon clusters under ultra-short laser pulses and three different temporal profile distributions of Gaussian and skewed Gaussian as near transform limited pulse, positively and negatively chirped laser pulse over range of intensities of 10^{14} – 10^{17} Wcm^{-2} . Argon cluster radius is considered 150 Å.

The optimal modifications are achieved by adjusting the optimal skew parameter for positive chirp in low intensity about 10^{14} Wcm^{-2} and negative chirp in high intensity laser pulses more than $2 \times 10^{15} \text{ Wcm}^{-2}$. The complex dynamics of laser-cluster interaction is modeled by three levels of the ionization, heating, and expansion of a cluster after irradiation by an intense laser pulse. Calculations successfully demonstrate the dependence of the particle density, the electron energy, and the radius of cluster with laser parameters and they can be improved by chirped laser pulses. The origin of the time is selected in a way in which E_{ext} maximum is located at $t = 0$ with FWHM of 40 fs.

Time evolution of the field inside the cluster and the external chirped intense pulse field according to Drude model are shown in Figure 1. This figure denotes that, by comparing the electric field inside the cluster and external laser pulse field, an enhanced internal field is achieved which leads to an enhanced ionization rate when the electron density sweeps through $3n_{\text{crit}}$. Figure 2 is presented in two dimensions in order to provide a better insight into the importance of the pulse duration and laser intensity effects on the produced electron energy and ion charge states.

Figure 2 elucidates the importance of the pulse duration and laser intensity by studying the manner of charge state and energy of emitted electrons for unchirped laser pulse. It shows that increasing laser intensity and laser pulse duration

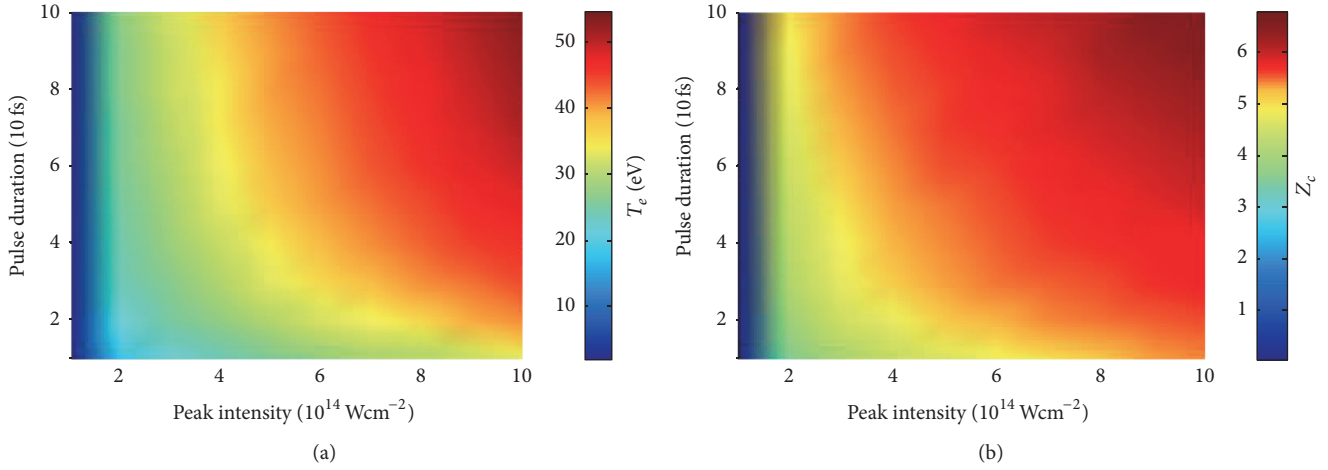


FIGURE 2: False color map of T_e (a) and Z_c (b) in Ar cluster at $t = 1.3\tau$ for an 825 nm wavelength pulse versus pump intensity and duration pulse $\tau = 40$ fs.

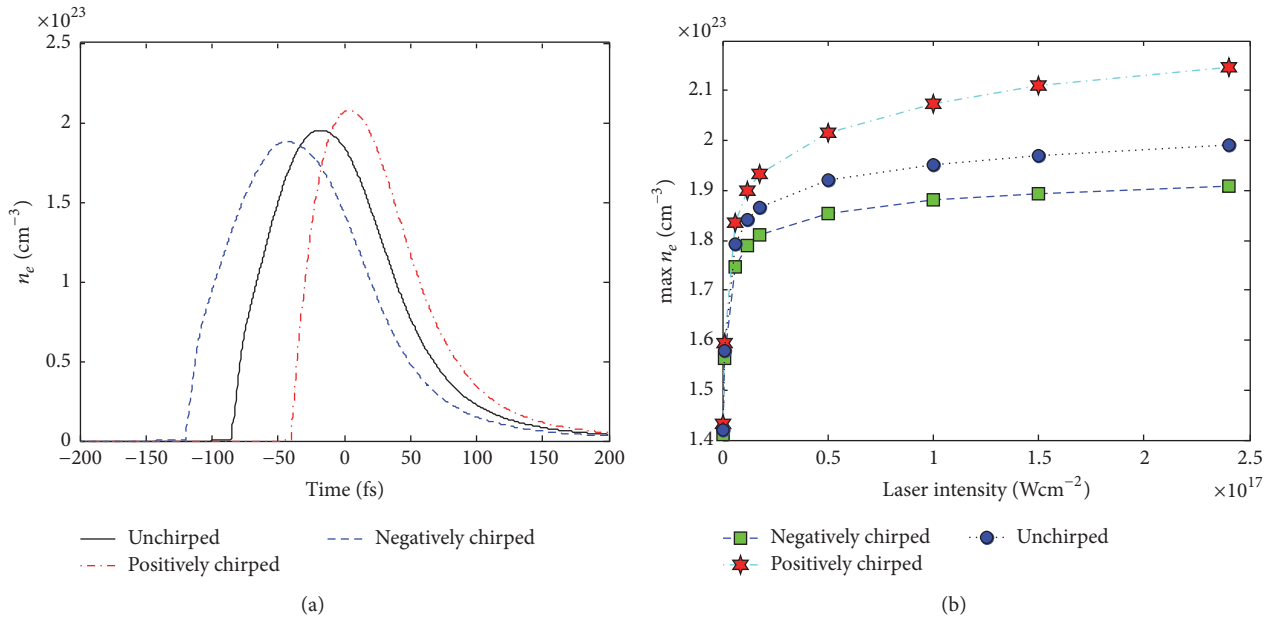


FIGURE 3: (a) Time evolution of the electron density with $1 \times 10^{17} \text{ Wcm}^{-2}$ laser intensity, 40 fs duration pulse, and wavelength of 825 nm. (b) The variations in the maximum electron density at the different laser pulse shapes in different laser intensities with 40 fs duration pulse and wavelength of 825 nm.

causes considerable increase of the electrons energy and ion charge states. This can have good impact on many laser-cluster interaction applications due to increasing the electron temperature. The aim is to study the effect of laser parameters including different shapes of laser pulses on the three levels of nanoplasma model. For a proper analysis of time-dependent cluster dynamics, the effective role of electron density in the first stage of this model is justified. According to nanoplasma approach, ionization processes play an important role to strip the electrons and ions to higher charge states. Time evolution of the electron density by 40 fs long near transform limited laser pulses, positively chirped pulses and negatively chirped pulse with peak laser intensity of 10^{17} Wcm^{-2} is presented in Figure 3.

Based on Figure 3, it is concluded that the ionization starts earlier for negatively chirped pulse in comparison to the unchirped and positively chirped pulses. However, the maximum density of electrons with positively chirped laser pulse is achieved. In addition to different mechanisms of tunneling ionization, collisional ionization, and field ionization, recombination of the electrons plays an important role in the electron density. Hence, the electron density will be low for negatively chirped pulse as a result of an early start tunneling ionization and the impact of other factors, which is demonstrated in Figure 3. Reducing the electron density with negatively chirped pulse indicates that strong heating is dominant. Furthermore, implementation of extended model including excited states, according to Figure 6(b) of Moll

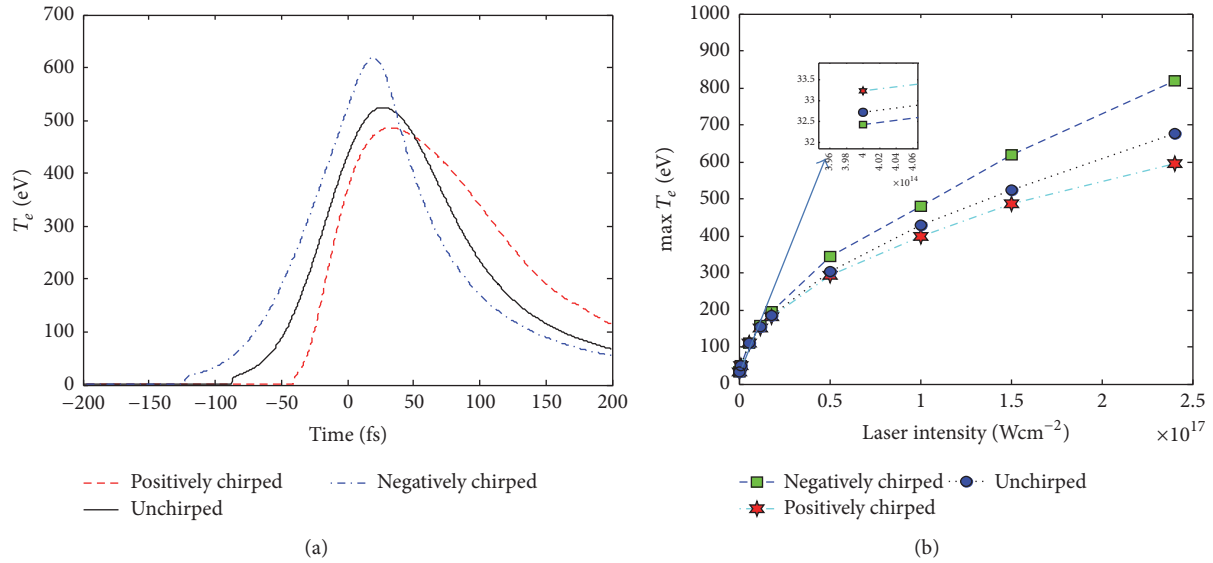


FIGURE 4: (a) Time evolution of the electron energy at the different laser pulse shapes with $1.5 \times 10^{17} \text{ Wcm}^{-2}$ laser intensity, 40 fs duration pulse, and wavelength of 825 nm. (b) The variations in the maximum electron energy at the different laser pulse shapes in different laser intensities with 40 fs duration pulse and wavelength of 825 nm.

et al.'s work [29], in comparison to the ground-state model, leads to 23% improvement in the electron density. It seems that, with considering both the excitation states and positively chirped pulse, the results can be further improved.

In order to obtain an estimate of the heating and enhancement of the acceleration of particles, the effects of laser intensity and the laser pulse shape as the main effective parameters have been investigated on the electron energy. Time evolution of electron energy for different laser pulse shapes with $1.5 \times 10^{17} \text{ Wcm}^{-2}$ laser intensity and the changes of electrons energy at different laser intensities are shown in Figure 4.

Indeed, in the time evolution of the laser excitation, free electrons and ions are created, and the heating of the produced nanoplasma leads to much higher charge states. Behind the laser pulse, the heating and ionization stop. Then the temperature of the system decreases and the system freezes out. Thus, the numbers of ions in the charge states remain constant. With increasing the peak intensity of the laser, the ionization dynamics is accelerated and shifted to smaller times t . When the cluster expands to the resonance condition with time, the laser pulse has already passed. Therefore, for longer duration pulses, the resonant absorption is near the peak of the pulse, which greatly enhances the cluster heating. Figure 4 shows that the enhancement occurs most intensively for negatively chirped pulses and the energy of electrons is improved up to 20% compared to the Gaussian pulse. However, the results of Figure 4(b) clearly demonstrate that the maximum energy of electrons can be improved by manipulating the character of laser intensity. The electron energy depends on the shape of the laser pulse at different intensities and is increased in condition of negatively chirped pulses when the applied laser pulse is more than $2 \times 10^{15} \text{ Wcm}^{-2}$. At low laser intensities, the positive

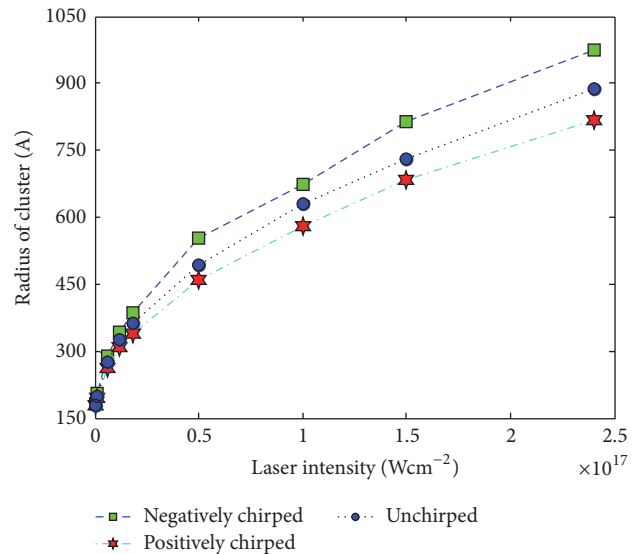


FIGURE 5: The variations in cluster size by changing the laser intensity at the different laser pulse shapes with 40 fs duration pulse and wavelength of 825 nm.

chirp is more effective due to the effect of intensity on the absorption coefficient according to (10). It should be realized that charging of cluster also causes a radial expansion of the cluster.

Variations of the cluster size by changing the laser intensity at the different laser pulse shapes are shown in Figure 5.

The effective role of the laser intensity in the interaction with clusters is interpreted for cluster to expansion in resonance condition. The dependence of bremsstrahlung

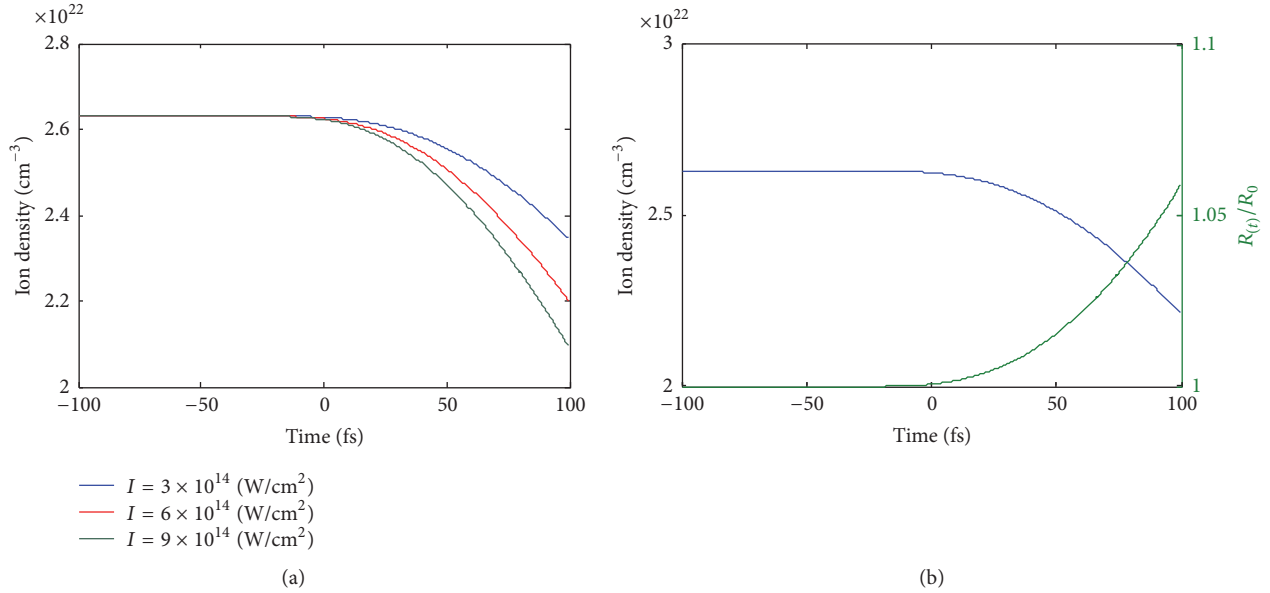


FIGURE 6: (a) Time evolution of the ion density of Ar cluster at the different laser intensities of 3×10^{14} Wcm⁻², 6×10^{14} Wcm⁻², and 9×10^{14} Wcm⁻². (b) Time evolution of the ion density with the size of cluster.

absorption on the laser intensity affects electron density, electron temperature, and recombination, resulting in 18% further expansion of the cluster for the negative chirp in comparison to the positive chirp. When the negatively chirped laser pulse interacts with a cluster, ionization starts earlier and heating and expansion process occur quickly and the radius of the cluster will be greater than other states. The density of cluster ions due to cluster expansion and acceleration of ions is declined and followed by enhancing the radius of the cluster. The charge state, ion density, and expanding cluster radius are challenging. To obtain the time-dependent cluster radius manner, time evolution of the ion density with the size of cluster at different laser intensities is shown in Figure 6.

From Figure 6, it is concluded that, due to cluster expansion and the ejection of the ions from the cluster, the ions density of cluster decreases with increases in the laser intensities. By increasing the laser intensity, energy absorption in cluster is enhanced and leads to the generation of hot electrons. High-energy electrons and ions are ejected and this can reduce the density of cluster ions. As the ion density decreases, the cluster size increases, which is seen from the time needed to reach the asymptotic value. It is more than 5% increase for about 25% decrease of the ion density. Another interesting point of this research work is investigating the role of chirped laser pulses in laser-cluster interaction in various pulse durations.

Figure 7 shows that, in short pulse duration, high-energy electrons are mainly generated as a result of cluster interaction with positively chirped laser pulses, and for the long laser pulse durations, the role of negatively chirped laser pulses is more effective. This process is due to the effective parameters on the electron temperature as is clarified in (10).

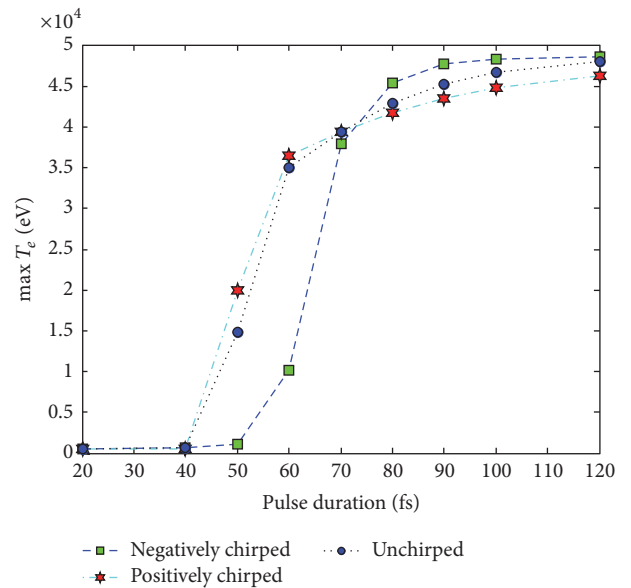


FIGURE 7: The variations in maximum energy of electrons at the positively and negatively chirped laser pulse as a function of pulse durations with 2×10^{17} Wcm⁻² laser intensity and wavelength of 825 nm.

4. Conclusion

In the present work, based on a modified theoretical executive model, behavior of complex dynamics of laser-Argon cluster interaction and its dependence on the laser pulse chirp is analyzed. This useful proposed theoretical model can properly explain the reported experimental results. This proposed theoretical model can properly explain the reported experimental results. In order to clarify the laser-cluster interaction, electron and ion density, electron energy,

and radius of cluster are modified by manipulating the characters of laser fields, such as intensity, pulse duration, and chirp parameter by using nanoplasma model. It should be noted that, besides the dependence of the interaction process into the mentioned parameters, there is about 20% improvement for the energy of electrons which are evaluated by negatively chirped femtosecond laser pulse. Based on this model, the dependence of bremsstrahlung absorption on laser intensity in electron density, electron temperature, and recombination indicates that 20% improvement is made for energy of electrons and 18% further expansion of cluster for the negative chirp in comparison to the positive chirp. Based on the recent researches [29], with implementation of extended model including excited states in comparison to the ground-state model, the ionization dynamics is accelerated, and higher ionic charge states are reached at the end of the laser-cluster interaction. By applying the results of this study, significant improvement occurs in the electron density and total energy.

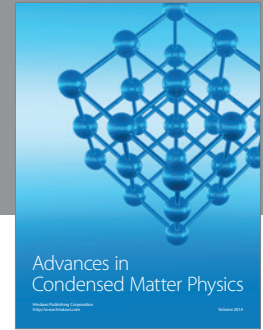
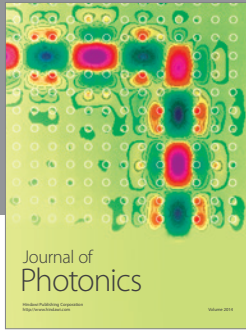
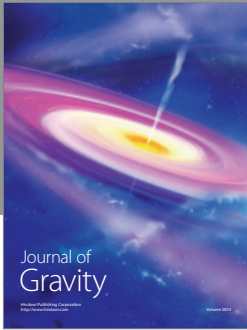
Competing Interests

The authors declare that they have no competing interests.

References

- [1] D. Strickland and G. Mourou, "Compression of amplified chirped optical pulses," *Optics Communications*, vol. 56, no. 3, pp. 219–221, 1985.
- [2] E. Irani, S. K. Sadighi, S. Zare, and R. Sadighi-Bonabi, "Laser-induced photo transmutation of ^{126}Sn —a hazardous nuclear waste product-into short-lived nuclear medicine of ^{125}Sn ," *Energy Conversion and Management*, vol. 64, pp. 466–472, 2012.
- [3] V. Malka and S. Fritzler, "Electron and proton beams produced by ultra short laser pulses in the relativistic regime," *Laser and Particle Beams*, vol. 22, no. 4, pp. 399–405, 2004.
- [4] N. A. M. Hafz, T. M. Jeong, I. W. Choi et al., "Stable generation of GeV-class electron beams from self-guided laser-plasma channels," *Nature Photonics*, vol. 2, no. 9, pp. 571–577, 2008.
- [5] T. Toncian, M. Amin, M. Borghesi et al., "Properties of a plasma-based laser-triggered micro-lens," *AIP Advances*, vol. 1, no. 2, Article ID 022142, 2011.
- [6] R. Sadighi-Bonabi and S. H. Rahmatallahpur, "Potential and energy of the monoenergetic electrons in an alternative ellipsoid bubble model," *Physical Review A*, vol. 81, no. 2, Article ID 023408, 2010.
- [7] L. M. Chen, M. Kando, M. H. Xu et al., "Study of X-ray emission enhancement via a high-contrast femtosecond laser interacting with a solid foil," *Physical Review Letters*, vol. 100, no. 4, Article ID 045004, 2008.
- [8] V. Arora, P. A. Naik, J. A. Chakera, S. Bagchi, M. Tayyab, and P. D. Gupta, "Study of 1-8 keV K- α X-ray emission from high intensity femtosecond laser produced plasma," *AIP Advances*, vol. 4, Article ID 047106, 2014.
- [9] M. D. Feit, J. C. Garrison, and A. M. Rubenchik, "Short pulse laser propagation in underdense plasmas," *Physical Review E*, vol. 53, no. 1, pp. 1068–1083, 1996.
- [10] H. Omi, T. Tawara, and M. Tateishi, "Real-time synchrotron radiation X-ray diffraction and abnormal temperature dependence of photoluminescence from erbium silicates on SiO_2/Si substrates," *AIP Advances*, vol. 2, no. 1, Article ID 012141, 2012.
- [11] K. W. D. Ledingham, P. McKenna, and R. P. Singhal, "Applications for nuclear phenomena generated by ultra-intense lasers," *Science*, vol. 300, no. 5622, pp. 1107–1111, 2003.
- [12] S. Rasti, E. Irani, and R. Sadighi-Bonabi, "Efficient photodissociation of CH_4 and H_2CO molecules with optimized ultrashort laser pulses," *AIP Advances*, vol. 5, no. 11, Article ID 117105, 2015.
- [13] A. M. Koushki, M. Mohsen-Nia, R. Sadighi-Bonabi, and E. Irani, "Ionization dynamics of orbitals and high-harmonic generation of N_2 and CO molecules at the various XC potentials by TD-DFT," *Computational and Theoretical Chemistry*, vol. 1095, pp. 104–111, 2016.
- [14] H. A. Navid, E. Irani, and R. Sadighi-Bonabi, "The effect of ultraviolet lasers on conversion of methane into higher hydrocarbons," *Laser and Particle Beams*, vol. 31, no. 3, pp. 481–486, 2013.
- [15] B. Cui, B. Tang, R. Ma et al., "Reliability test of an electron cyclotron resonance ion source for accelerator driven subcritical system," *Review of Scientific Instruments*, vol. 83, no. 2, Article ID 02A321, 2012.
- [16] T. Z. Zhan, C. N. Xu, H. Yamada et al., "Beam profile indicator for swift heavy ions using phosphor afterglow," *AIP Advances*, vol. 2, no. 3, Article ID 032116, 2012.
- [17] E. Irani, S. Zare, H. A. Navid, Z. Dehghani, and R. Sadighi-Bonabi, "The effect of intense short pulse laser shapes on generating of the optimum wakefield and dissociation of methane molecule," *Laser and Particle Beams*, vol. 30, no. 3, pp. 357–367, 2012.
- [18] F. N. Beg, K. Krushelnick, C. Gower et al., "Table-top neutron source for characterization and calibration of dark matter detectors," *Applied Physics Letters*, vol. 80, no. 16, pp. 3009–3011, 2002.
- [19] V. D. Zvorykin, A. O. Levchenko, A. V. Shutov, E. V. Solomina, N. N. Ustinovskii, and I. V. Smetanin, "Long-distance directed transfer of microwaves in tubular sliding-mode plasma waveguides produced by KrF laser in atmospheric air," *Physics of Plasmas*, vol. 19, no. 3, Article ID 033509, 2012.
- [20] N. L. Kugland, B. Aurand, C. G. Brown et al., "Demonstration of a low electromagnetic pulse laser-driven argon gas jet x-ray source," *Applied Physics Letters*, vol. 101, no. 2, Article ID 024102, 2012.
- [21] L. Nikzad, R. Sadighi-Bonabi, Z. Riazi, Z. M. Mohammadi, and F. Heydarian, "Simulation of enhanced characteristic x rays from a 40-MeV electron beam laser accelerated in plasma," *Physical Review Accelerators and Beams*, vol. 15, no. 2, Article ID 021301, 10 pages, 2012.
- [22] M. Shirozhan, M. Moshkelgosha, and R. Sadighi-Bonabi, "The effects of circularly polarized laser pulse on generated electron nano-bunches in oscillating mirror model," *Laser and Particle Beams*, vol. 32, no. 2, pp. 285–293, 2014.
- [23] B. Shokri, A. R. Niknam, and V. Krainov, "Cluster structure effects on the interaction of an ultrashort intense laser field with large clusters," *Laser and Particle Beams*, vol. 22, no. 1, pp. 13–18, 2004.
- [24] L. Zhang, L.-M. Chen, W.-M. Wang et al., "Electron acceleration via high contrast laser interacting with submicron clusters," *Applied Physics Letters*, vol. 100, no. 1, Article ID 014104, 2012.

- [25] T. Ditmire, T. Donnelly, A. M. Rubenchik, R. W. Falcone, and M. D. Perry, "Interaction of intense laser pulses with atomic clusters," *Physical Review A*, vol. 53, no. 5, pp. 3379–3402, 1996.
- [26] S. Micheau, H. Jouin, and B. Pons, "Modified nanoplasma model for laser-cluster interaction," *Physical Review A*, vol. 77, no. 5, Article ID 053201, 2008.
- [27] E. S. Dodd and D. Umstadter, "Coherent control of stimulated Raman scattering using chirped laser pulses," *Physics of Plasmas*, vol. 8, no. 8, pp. 3531–3534, 2001.
- [28] R. J. Levis, G. M. Menkir, and H. Rabitz, "Selective bond dissociation and rearrangement with optimally tailored, strong-field laser pulses," *Science*, vol. 292, no. 5517, pp. 709–713, 2001.
- [29] M. Moll, M. Schlanges, Th. Bornath, and V. P. Krainov, "Influence of excitation and deexcitation processes on the dynamics of laser-excited argon clusters," *Physical Review A*, vol. 91, no. 3, Article ID 033405, 2015.
- [30] Y. Fukuda, K. Yamakawa, Y. Akahane et al., "Optimized energetic particle emissions from Xe clusters in intense laser fields," *Physical Review A*, vol. 67, no. 6, Article ID 061201, 2003.
- [31] I. Last and J. Jortner, "Nuclear fusion induced by coulomb explosion of heteronuclear clusters," *Physical Review Letters*, vol. 87, no. 3, Article ID 033401, 2001.
- [32] C. Rose-Petrucci, K. J. Schafer, K. R. Wilson, and C. P. J. Barty, "Ultrafast electron dynamics and inner-shell ionization in laser driven clusters," *Physical Review A—Atomic, Molecular, and Optical Physics*, vol. 55, no. 2, pp. 1182–1190, 1997.
- [33] D. Brunner, H. Angerer, E. Bustarret et al., "Optical constants of epitaxial AlGa_N films and their temperature dependence," *Journal of Applied Physics*, vol. 82, no. 10, pp. 5090–5096, 1997.
- [34] M. V. Ammosov, N. B. Delone, and V. P. Krainov, "Tunnel ionization of complex atoms and of atomic ions in an alternating electromagnetic field," *Soviet Physics*, vol. 64, no. 6, p. 1191, 1986.
- [35] W. Lotz, "Electron-impact ionization cross-sections for atoms up to Z=108," *Zeitschrift für Physik*, vol. 232, no. 2, pp. 101–107, 1970.
- [36] J. S. Zweiback, *Resonance effects in laser cluster interactions [Ph.D. thesis]*, University of California, Davis, Calif, USA, 1999.
- [37] A. V. Gurevich and L. P. Pitaevskii, "Recombination coefficient in a dense low-temperature plasma," *Soviet Physics—Journal of Experimental and Theoretical Physics*, vol. 19, no. 4, p. 870, 1964.
- [38] J. D. Jackson, *Classical Electrodynamics*, Wiley-Interscience, New York, NY, USA, 1975.
- [39] O. F. Kostenko and N. E. Andreev, "Heating and ionization of metal clusters in the field of an intense femtosecond laser pulse," *Plasma Physics Reports*, vol. 33, no. 6, pp. 503–509, 2007.
- [40] A. F. Haught, W. B. Ard, W. J. Fader et al., United Aircraft Research Labs, East Hartford, Conn, USA, pp. 391–398, 1975.



Hindawi

Submit your manuscripts at
<http://www.hindawi.com>

